# Journal Pre-proof

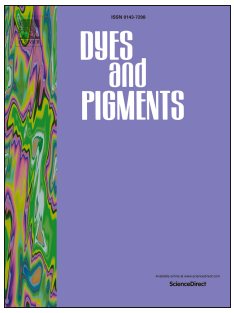


Design strategy of multifunctional and high efficient hydrogen sulfide NIR fluorescent probe and its application in *vivo*

Keyan Zhou, Yutao Yang, Tingting Zhou, Ming Jin, Caixia Yin

PII: S0143-7208(20)31598-9

DOI: https://doi.org/10.1016/j.dyepig.2020.108901

Reference: DYPI 108901

To appear in: *Dyes and Pigments*

Received Date: 21 July 2020

Revised Date: 15 September 2020

Accepted Date: 28 September 2020

Please cite this article as: Zhou K, Yang Y, Zhou T, Jin M, Yin C, Design strategy of multifunctional and high efficient hydrogen sulfide NIR fluorescent probe and its application in *vivo*, *Dyes and Pigments*, https://doi.org/10.1016/j.dyepig.2020.108901.

This is a PDF file of an article that has undergone enhancements after acceptance, such as the addition of a cover page and metadata, and formatting for readability, but it is not yet the definitive version of record. This version will undergo additional copyediting, typesetting and review before it is published in its final form, but we are providing this version to give early visibility of the article. Please note that, during the production process, errors may be discovered which could affect the content, and all legal disclaimers that apply to the journal pertain.

© 2020 Elsevier Ltd. All rights reserved.

Journal Pre-proof

# Author contributions

Keyan Zhou carried out synthesis and spectrometry.
Tingting Zhou and Ming Jin carried out cell imaging and mice imaging.
Yutao Yang and Caixia Yin's idea and writing.

Journal Pre-proof

# Abstract Graphic

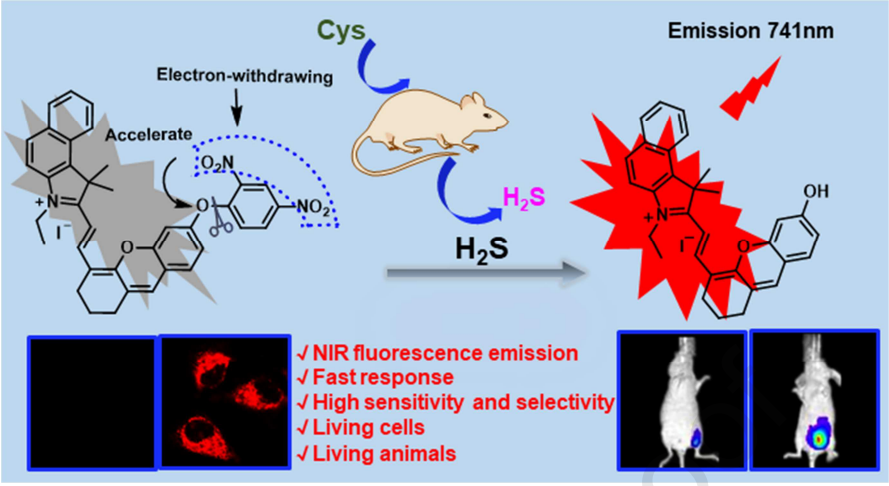


Journal Pre-proof

Journal Pre-proof

# Design strategy of multifunctional and high efficient hydrogen sulfide NIR fluorescent probe and its application in *vivo*

Keyan Zhou, [a] Yutao Yang, [a*] Tingting Zhou, [a] Ming Jin, [a] Caixia Yin[b*]

[a] Key Laboratory of Medicinal Chemistry, and Molecular Diagnosis of the Ministry of Education, Key Laboratory of Chemical Biology of Hebei Province, College of Chemistry & Environmental Science, Key Laboratory of Chemical Biology of Hebei Province, Hebei University, Baoding 071002, China

*E-mail: yutaoyang2016@163.com.

[b] Key Laboratory of Chemical Biology and Molecular Engineering of Ministry of Education, Institute of Molecular Science, Shanxi University, Taiyuan 030006, China

*E-mail: yincx@sxu.edu.cn.

## Abstract

With the improvement of organic synthesis technology and the development of fluorescent probe, more and more fluorescent probes with excellent performance and versatility are required, so as to better realize their application value. High sensitivity, high selectivity, targetable and fast response NIR fluorescence probes are still needed for hydrogen sulfide precise detection. In this study, phenol containing 2, 4-dinitro group was selected as a strong electrophilic group to promote the nucleophilic substitution reaction. After the nucleophilic addition reaction between probe and hydrogen sulfide with delicate structure, strong nucleophile, 2, 4-dinitrophenol departure quickly and the NIR fluorophore was released, which showed fluorescence emission at 741 nm, and the probe detection limit for hydrogen sulfide was calculated as 96 nM. Interestingly, because of the positive charge in the hemiocyanine, the probe can locate efficiently in the mitochondria. This fluorescent probe with excellent performance was used to detect the endogenous levels of hydrogen sulfide in *vivo*. This work provides guidance for the design of multifunctional and high-performance fluorescent probes.

***Keywords:*** Fluorescent probe; Multifunctional; Efficient; Bioimaging; $H_2S$.

## 1. Introduction

Hydrogen sulfide ($H_2S$) is recently regarded as the third gas messenger molecule in addition to carbon monoxide (CO) and nitric oxide (NO). [1] $H_2S$ is not only widely exists in mammals, including humans, but also plays an important in numerous pathologic and physiologic processes.[2-5] $H_2S$ can be endogenously catalyzed by enzymes such as cystathionine-γ-lyase (CSE), cystathionine-β-synthase (CBS), and 3-mercapto-sulfurtransferase.[6-11] As an endogenous signal molecule, $H_2S$ is involved in vasodilation, angiogenesis, cell growth, neuromodulation, insulin signal inhibition, inflammation and other physiological functions.[12-18] Many physical diseases of diabetes, Alzheimer's disease, cirrhosis of the liver are now widely accepted as being induced or related to abnormal levels of hydrogen sulfide. Recently, the potential biological significance of $H_2S$ has attracted growing interest. As an effective detection approach, fluorescent probe has great development potential in visualizing $H_2S$ in biological systems due to the unique advantages of simple operation, fast response and excellent selectivity for $H_2S$. To date, various red emitted or NIR fluorescent probes for $H_2S$ have been developed, but their emission wavelengths are under 700 nm. [19-29] In recent years, some NIR fluorescent probes were reported which the emission wavelengths are beyond 700 nm. In 2018, Ai et al. developed a NIR fluorescent probe Imazide for $H_2S$ and the emission maxima was 733 nm.[30] Wang et al. developed a new fluorescent probe for $H_2S$ based on cyanine dyes and the emission wavelength centered at 830 nm.[31] These probes have made a perfect effect in detection of mitochondrial $H_2S$ in the living cells. However, the optical properties analysis was performed in the buffer solutions with 90% glycerol or the response time of probe to $H_2S$ is within 1 h. In 2019, Feng et al. developed a NIR fluorescent probe for $H_2S$ with the signal at 744 nm based nitrobenzoxadiazole ether. [32] Huang group developed a new probe DBT for detection of $H_2S$ with a significant "turn-on" fluorescence response at 716 nm.[33] Besides, the probes were successfully applied in imaging $H_2S$ in live cells and mice. They did not achieve detection of $H_2S$ in mitochondria as an important organelle of the cell playing a significant role in

pathophysiology. [34-37] Therefore, it is still need to develop some new types of fluorescent probes for $H_2S$.

With the above in mind, we focused on development of NIR mitochondrial targeting fluorescent probe for detection $H_2S$ to elucidate the function of hydrogen sulfide in mitochondria and the association between hydrogen sulfide and related diseases in mitochondria. It is worth noting that the key to design a mitochondria-targetable NIR fluorescent probe for $H_2S$ is to choose a mitochondrial targeting group, the near-infrared fluorophore and a specific response site for detection of $H_2S$. It is generally known that many kinds of cationic dyes, such as cyanine and rhodamine, possessing a positive charge, which can be well accumulated in the mitochondria of cells.[38] Thus, we choose the cyanine dye **Mito-OH** as the fluorophore, owing to its mitochondrial targeting and NIR emission. In addition, we used 2,4-dinitrophenyl (DNP) ether for reaction moiety because of its sensitivity and selectivity for $H_2S$ without the interference of biothiols.[39-45] Therefore, in this work, we designed and synthesis of **Mito-DNP** with NIR emission for detection of $H_2S$ on the basis of the thiolysis of dinitrophenyl ether via combinatorial chemistry (Scheme 1). After treatment of $H_2S$, **Mito-DNP** would occur $H_2S$-triggered thiolysis of dinitrophenyl ether to release **Mito-OH.** Moreover, the feasibility of **Mito-DNP** as a fluorescent probe to monitor the level of $H_2S$ was evaluated in the HepG2 cells and mice. These results might lead to better understand the roles of $H_2S$ in physiological processes.

## 2. Experimental

### *2.1 Reagents and apparatus*

Deionized water was used in the whole experiment and the chemicals were of analytical grade and used directly. The ultraviolet spectra and fluorescence spectra were measured using the Agilent Technologies UV-visible (Cary 60) and fluorescence spectrophotometer (Cary Eclipse). The spectra of $^{1}H$ NMR and $^{13}C$ NMR were recorded by BUXI-I NMR spectrometer (Wuhan Zhongke Niu-jin). The mass spectra

were recorded on ESI mode (Bruker Ultraflex Xtreme MALDI-TOF/TOF). Live cells imaging was observed with laser confocal microscopy (ZEISS LSM 880). Animal imaging was taken by the PerkinElmer IVIS Spectrum live animal imaging system.

*2.2 Synthesis of **Mito-DNP***

The synthesis route of **Mito-DNP** is summarized in Scheme 1. Fluorophore **Mito-OH** was synthesized according to previous research in our laboratory.[46] **Mito-OH** (0.29 g, 0.5 mmol) and 2,4-dinitrobromobenzene (0.25g, 1 mmol) were dissolved in dichloromethane (10 mL), then added the $K_2CO_3$ (0.21 g, 1.5 mmol) to the above solution and stirring at 25□ for 12 h. Next, after filtration, the solvent was evaporated to give a crude product and then it was isolated by silica gel chromatography ($CH_2Cl_2$: MeOH=30:1) to obtain a blue-purple solid (0.14 g, 39 %). M.p. >280□. $^1$H NMR (400 MHz, $CDCl_3$) δ (ppm): 8.82 (d, *J* = 2.2 Hz, 1H), 8.73 (d, *J* = 12.0 Hz, 1H, 8.48 (d, *J* = 7.2 Hz, 1H), 8.22-8.14 (m, 1H), 8.04 (d, *J* = 8.0 Hz, 1H), 7.98 (d, *J* = 8.0 Hz, 2H), 7.71 (d, *J* = 8.6 Hz, 1H), 7.67-7.61 (m, 1H), 7.21 (d, *J* = 5.8 Hz, 3H), 7.68 (d, *J* = 8.0 Hz, 1H), 7.69 (d, *J* = 17.2 Hz, 1H), 4.69 (s, 1H), 4.48 (s, 2H), 2.80-2.72 (m, 4H), 2.04 (s, 6H), 1.93 (s, 2H), 1.60 (d, *J* = 4.0 Hz, 3H); $^{13}$C NMR (100 MHz, $CDCl_3$) δ (ppm): 179.2, 159.1, 155.4, 154.6, 153.7, 145.3, 142.1, 139.7, 138.1, 136.6, 133.0, 131.5, 130.4, 129.7, 128.9, 128.7, 128.2, 127.5, 126.9, 126.6, 122.4, 121.9, 120.1, 116.7, 115.5, 111.6, 108.1, 105.5, 52.7, 42.2, 33.6, 29.6, 27.6, 20.1, 13.5. HRMS (ESI, *m/z*): Calcd for $C_{37}H_{32}N_3O_6^+$ ([M]$^+$) 614.2286, found: 614.2284.

*<Inserted Scheme 1>*

*2.3 General preparation for optical measurements*

The stock solution of **Mito-DNP** and various analytes were prepared in DMSO and deionized water respectively. All spectra were measured in DMF-PBS (10 mM, pH 7.4, v:v =1:1) buffer solution. For the measurements, excitation wavelength was 680 nm, the slit widths were 5 nm and the voltage was fixed at 600V.

*2.4 Cell culture and imaging*

The HepG2 cells were grown in DMEM medium supplemented with 10 % FBS, 1 % of penicillin at 37 °C under 5 % $CO_2$. For imaging of $H_2S$ in living cells, HepG2 cells were incubated with 10 μM of **Mito-DNP** for 30 min, and then imaged. Meanwhile, for imaging of exogenous $H_2S$ in live cells, after being pretreated with $Na_2S$ (20, 50, 100 μM) for 30 min, following by 10 μM of **Mito-DNP**. For imaging of endogenous $H_2S$, three groups of experiments were carried out. The cells were pretreated with an inhibitor of $H_2S$ production by cystathionine γ-lyase propargylglycine (PAG), cysteine (Cys) or PAG and Cys, then were hatched with **Mito-DNP** (10 μM) subsequently.

*2.5 Imaging of $H_2S$ in vivo*

BALB/c Nude Mice were purchased from Beijing Spaifu Biotechnology Co., Ltd. and utilized as biological models. The mice were split into four groups. As the control group, the mice were injected with only **Mito-DNP**, the other three groups of mice were injected with $Na_2S$, Cys or Cys and PAG respectively, following by injection with **Mito-DNP**. All injections were performed intraperitoneally, and images were recorded by the PerkinElmer IVIS Spectrum live animal imaging system.

## 3. Results and discussion

*3.1. Response of **Mito-DNP** to $H_2S$*

The sensing properties of **Mito-DNP** for $H_2S$ were initially investigated. The absorption and fluorescence emission spectra were recorded in PBS buffer (10 mM, pH 7.4) with 50 % DMF. Figure 1 depicted that the probe **Mito-DNP** exhibited an absorbance peak at around 609 nm and a fluorescence emission at 741 nm with addition of $H_2S$. Herein, it will helpful for further fluorescence imaging of $H_2S$ in organisms. Subsequently, the absorption and fluorescence titration of **Mito-DNP** towards $H_2S$ were studied (Figure 2). In the absorbance spectrum, the probe **Mito-DNP** (10 μM) showed maximum absorption peak at 609 nm. When the $Na_2S$ (100 μM, the source for $H_2S$) was added, two new absorption peaks at 718 nm and 380 nm significantly increased, while the absorption peak at 609 nm gradually decreased. Corresponding to the fluorescence spectrum, the free probe **Mito-DNP** had no fluorescence, however, the fluorescence intensity of **Mito-DNP** remarkably

increased at 741 nm after adding 100 μM of $Na_2S$ due to the thiolysis of dinitrophenyl ether and the **Mito-OH** to release. The fluorescence intensity of 741 nm reached saturation and increased nearly by 20-fold. In addition, the detection limit of **Mito-DNP** for $H_2S$ was calculated as 0.096 μM by S/N =3 method. [47] Moreover, the kinetic analysis was also investigated and the fluorescence intensity stabilized in 5 min after adding of $H_2S$, indicating that **Mito-DNP** has a fast response to $H_2S$ (Figure S1). Futhermore, such large emission wavelengths of **Mito-DNP** were superior to some reported probes for $H_2S$ (Table S1) and it might be an excellent candidate for detecting $H_2S$ in biological systems. Beyond that, the effects of pH value on the fluorescence response of **Mito-DNP** to $H_2S$ was also studied and discussed. The free probe **Mito-DNP** was no fluorescence in the pH value of 3-11, but obvious fluorescence enhancement of **Mito-DNP** at 741nm in the pH value of 6-9 with $H_2S$ (Figure S2). Thus, **Mito-DNP** could function at physiological pH.

*<Inserted Figure 1>*

*<Inserted Figure 2>*

*3.2 The Selectivity of probe **Mito-DNP***

Selectivity is an essential factor for fluorescent probe. Thus, the specific selectivity of **Mito-DNP** for $H_2S$ was demonstrated. We performed interference analysis of fluorescence spectra (Figure 3). Under the same conditions, some analytes including $H_2S$, $H_2O_2$, various anions ($F^-$, $SCN^-$, $I^-$, $Br^-$, $HSO_3^-$, $SO_4^{2-}$, $CO_3^{2-}$, $NO_3^-$, $NO_2^-$, $Cl^-$, $N_3^-$, $ClO^-$), biothiols (Hcy, Cys, GSH) and various cations ($K^+$, $Ba^{2+}$, $Ca^{2+}$, $Mg^{2+}$, $Al^{3+}$, $Cu^{2+}$) were added into the PBS-DMF solution containing 10 μM **Mito-DNP** respectively. None of these species led to significant fluorescence response and only $H_2S$ induced obvious fluorescent turn-on changes. The results showed that the probe did not react with any one of these analytes. In addition, the competitive experiments were also performed and the results showed that the probe **Mito-DNP** has the anti-interference ability for the detection of $H_2S$ (Figure S3). Therefore, it demonstrated that **Mito-DNP** has a high selectivity for $H_2S$, confirming that the

dinitrophenyl ether can selectively react with $H_2S$ in the biological systems.

*<Inserted Figure 3>*

*3.3 Proposed mechanism*

The proposed sensing mechanism of **Mito-DNP** for $H_2S$ was shown in Scheme 2. The nucleophilic $HS^-$ attacked directly on the dinitrophenyl ether of **Mito-DNP** and thereby led to a rapid release of the fluorescent **Mito-OH**. The proposed mechanism was further confirmed by analyzing mass spectra changes of **Mito-DNP** before and after the addition of $Na_2S$. Upon addition of $Na_2S$ to the chromatographic methanol solution containing **Mito-DNP** and then was subjected to HRMS analysis. The results showed a peak at 448.2274, which could be ascribed to the released **Mito-OH** ($[M]^+$, calcd m/z=448.2271) (Figure S4). It revealed that $H_2S$ triggered thiolysis of dinitrophenyl ether of **Mito-DNP** to release **Mito-OH** indeed happened and proved the mechanism we speculated.

*<Inserted Scheme 2>*

*3.4 Cellular $H_2S$ Analysis*

Encouraged by above excellent performance of probe **Mito-DNP**, the capability of probe **Mito-DNP** for imaging $H_2S$ in biological systems was explored. Initially, the cytotoxicity of probe **Mito-DNP** was determined by the MTT assay. The results suggested that the probe has negligible toxicity to HepG2 within 20 μM (Figure S5). The cellular distribution of **Mito-DNP** was further measured whether **Mito-DNP** could detect $H_2S$ in living cells and localize in mitochondria by commercial mitochondria labeling agent Mito-Tracker Green. Figure 4 indicated that **Mito-DNP** could easily penetrate cell membrane and aggregate in mitochondria and calculated the overlap coefficient is about 0.963.

To further investigate the potential capability of **Mito-DNP** for quantitative detection of $H_2S$ in HepG2 cells. First, incubation of the HepG2 cells with **Mito-DNP** showed weak fluorescence. However, the HepG2 cells were pretreated with $Na_2S$ (20, 50, 100 μM), then incubated with **Mito-DNP**, the enhanced fluorescence was observed (Figure 5a), indicating that **Mito-DNP** could image exogenous $H_2S$ in live cells with outstanding performance. Figure 5b depicted that the cells were hatched with only **Mito-DNP** (10 μM) and showed weak fluorescence. When cells were pre-incubated with PAG for 30 min, following by **Mito-DNP** (10 μM), the fluorescence signal decreased. However, the HepG2 cells were treated with Cys (an inductor of endogenous $H_2S$), a stronger fluorescence has been observed. Furthermore, when the HepG2 cells were incubated with PAG and Cys, then treated with **Mito-DNP**, the fluorescence was inhibited to some extent. It exhibited that **Mito-DNP** could mornitor $H_2S$ fluctuations in living cells. All the above results demonstrated that **Mito-DNP** could be used to track $H_2S$ in cells.

*<Inserted Figure 4>*

*<Inserted Figure 5>*

*3.5 Living Animals $H_2S$ analysis*

With the above-mentioned results, the capability of **Mito-DNP** to image $H_2S$ in animals was also evaluated. For the experiment, we selected the four-week old athymic nude mice for the research. The mice were divided into four groups and induced by intraperitoneal injection. For the control group, the mouse was anesthetized by urethane, then injected with probe **Mito-DNP** (Figure 6A). In a second group, the mouse was pre-treated with Cys and injected with **Mito-DNP** in the same place, the higher fluorescence intensity was noticed compared with the control group (Figure 6B). Similarly, after injection of Cys, then the mouse were treated PAG and **Mito-DNP**, the fluorescence intensity weakened significantly (Figure 6C). However, the mice was injected with $Na_2S$ and **Mito-DNP**, the obvious fluorescence

was also observed (Figure 6D). Experimental data clearly indicated that **Mito-DNP** could detect exogenous and endogenous $H_2S$ in mice.

*<Inserted Figure 6>*

## 4. Conclusion

In conclusion, we designed and developed a new NIR fluorescent probe **Mito-DNP** on the basis of thiolysis of dinitrophenyl ether (DNP) for selective detection of $H_2S$ over various analytes and biothiols via turn-on fluorescence emission. Due to lower detection limit (96 nM) and application in a wide pH range, the probe **Mito -DNP** could be specifically triggered by endogenous $H_2S$ in HepG2 cells. Moreover, the probe is also suitable for tracking endogenous and exogenous of $H_2S$ in mice. Therefore, probe **Mito-DNP** is helpful for detection of $H_2S$ in organisms and has the application of a large space in the disease diagnosis.

**Acknowledgments**

This work was supported by the Natural Science Foundation of China (21807021), the Hebei Province Natural Science Foundation (B2020201074) advanced talents incubation program of the hebei university and the Priority Strategy Project of Key Laboratory of Medicinal Chemistry and Molecular Diagnosis of Ministry of Education (ts2019004).

Journal Pre-proof

## References

[1] Ma Y, Su H, Kuang X, Li XY, Zhang TT, Tang B. Heterogeneous nano metalorganic framework fluorescence probe for highly selective and sensitive detection of hydrogen sulfide in living cells. Anal Chem 2014;86:11459-63.

[2] Pandey SK, Kim KH, Tang KT. A review of sensor-based methods for monitoring hydrogen sulfide. Trac Trends Anal Chem 2012;32:87-99.

[3] Yang MW, Fan JL, Du JJ, Peng XJ. Small-molecule fluorescent probes for imaging gaseous signaling molecules: current progress and future implications. Chem Sci 2020;11:5127-41.

[4] Gao P, Pan W, Li N, Tang B. Fluorescent probes for organelle-targeted bioactive species imaging. Chem Sci 2019;10:6035-71.

[5] Kamoun P. Endogenous production of hydrogen sulfide in mammals. Amino Acids 2004;26:243-54.

[6] Hammers MD, Taormina MJ, Cerda MM, Montoya LA, Seidenkranz DT, Parthasarathy R, Pluth MD. A bright fluorescent probe for $H_2S$ enables analyte-responsive, 3D imaging in live zebrafish using light sheet fluorescence microscopy. J Am Chem Soc 2015;137:10216-23.

[7] Zhang X, Tan HQ, Yan YC, Hang YD, Yu FT, Qu X, Hua JL. Targetable N-annulated perylene-based colorimetric and ratiometric near-infrared fluorescent probes for the selective detection of hydrogen sulfide in mitochondria, lysosomes, and serum. J Mater Chem B 2017;5:2172-80.

[8] Gu B, Su W, Huang LY, Wu CY, Duan XL, Li YQ, Xu H, Huang Z, Li HT, Yao SZ. Real-time tracking and selective visualization of exogenous and endogenous hydrogen sulfide by a near-infrared fluorescent probe. Sens Actuators B 2018;255:2347-55.

[9] Liu C, Pan J, Li S, Zhao Y, Wu LY, Berkman CE, Whorton AR, Xian M. Capture and visualization of hydrogen sulfide by a fluorescent probe. Angew Chem Int Ed 2011;50:10327-9.

Journal Pre-proof

[10] Huang ZJ, Ding SS, Yu DH, Huang FH, Feng GQ. Aldehyde group assisted thiolysis of dinitrophenyl ether: a new promising approach for efficient hydrogen sulfide probes. Chem Commun 2014;50:9185-7.

[11] Ding SS, Feng WY, Feng GQ. Rapid and highly selective detection of $H_2S$ by nitrobenzofurazan(NBD) ether-based fluorescent probes with an aldehyde group. Sens Actuators B 2017;238:619-25.

[12] Cao XW, Lin WY, Zheng KB, He LW. A near-infrared fluorescent turn-on probe for fluorescence imaging of hydrogen sulfide in living cells based on thiolysis of dinitrophenyl ether. Chem Commun 2012;48:10529-31.

[13] Liu Y, Feng GQ. A visible light excitable colorimetric and fluorescent ESIPT probe for rapid and selective detection of hydrogen sulfide. Org Biomol Chem 2014;12:438-45.

[14] Lavu M, Bhushan S, Lefer DJ. Hydrogen sulfide-mediated cardioprotection: mechanisms and therapeutic potential. Clin Sci 2011;120:219-29.

[15] Lefer DJ. A new gaseous signaling molecule emerges: cardioprotective role of hydrogen sulfide. Natl Acad Sci U S A 2007;104:17907-8.

[16] Yang G, Wu L, Jiang B, Yang W, Qi J, Cao K, Meng Q, Mustafa AK, Mu W, Zhang S, Snyder SH, Wang R. $H_2S$ as a physiologic vasorelaxant: hypertension in mice with deletion of cystathionine γ-lyase. Science 2008;322:587-90.

[17] Zhao Q, Huo FJ, Kang J, Zhang YB, Yin CX. A novel FRET-based fluorescent probe for the selective detection of hydrogen sulfide ($H_2S$) and its application for bioimaging. J Mater Chem B 2018;6:4903-8.

[18] Hong JX, Feng WY, Feng GQ. Highly selective near-infrared fluorescent probe with rapid response,remarkable large Stokes shift and bright fluorescence for $H_2S$ detection in living cells. Sens Actuators B 2018;262:837-44.

[19] Feng SM, Xia QF, Feng GQ. Iminocoumarin-based red to near-infrared fluorescent turn-on probe with a large Stokes shift for imaging $H_2S$ in living cells and animals. Dyes Pigments 2019;163:447-53.

Journal Pre-proof

[20] Hong JX, Zhou EB, Gong SY, Feng GQ. A red to near-infrared fluorescent probe featuring a super large Stokes shift for light-up detection of endogenous $H_2S$. Dyes Pigments 2019;160:787-93.

[21] Jin YL, Liu R, Zhan ZX, Lv Y. Fast response near-infrared fluorescent probe for hydrogen sulfide in natural waters. Talanta 2019;202:159-64.

[22] Zhao ZS, Cao LX, Zhang T, Hu R, Wang SQ, Li SY, Li Y, Yang GQ. Novel reaction-based fluorescence probes for the detection of hydrogen sulfide in living cells. ChemistrySelect 2016;1:2581-5.

[23] Zhao XJ, Li YT, Jiang YR, Yang BQ, Liu C, Liu ZH. A novel "turn-on" mitochondria-targeting near-infrared fluorescent probe for $H_2S$ detection and in living cells imaging. Talanta 2019;197:326-33.

[24] Wei C, Zhu Q, Liu WW, Chen WB, Xi Z, Yi L. NBD-based colorimetric and fluorescent turn-on probes for hydrogen sulfide. Org Biomol Chem 2014;12:479-85.

[25] Men JX, Yang XJ, Zhang HB, Zhou JP. A near-infrared fluorescent probe based on nucleophilic substitution–cyclization for selective detection of hydrogen sulfide and bioimaging. Dyes Pigments 2018;153:206-12.

[26] Huang XT, Liu HY, Zhang JW, Xiao BR, Wu FX, Zhang YY, Tan Y, Jiang YY. A novel near-infrared fluorescent hydrogen sulfide probe for live cells and tissues imaging. New J Chem 2019;43:6848-55.

[27] Ma T, Huo FJ, Yin CY. A 'naked-eye' ratiometric and NIR fluorescent detection for hydrogen sulphide with quick response and high selectivity for and its bioimaging. Dyes Pigments 2019;165:31-7.

[28] Lin XF, Lu XH, Zhou JL, Ren H, Dong XC, Zhao WL, Chen ZJ. Instantaneous fluorescent probe for the specific detection of $H_2S$. Spectrochim Acta A 2019;213:416-22.

[29] Wu Q, Yin CX, Wen Y, Zhang YB, Huo FJ. An ICT lighten ratiometric and NIR fluorogenic probe to visualize endogenous/exogenous hydrogen sulphide and imaging in mice. Sens Actuators B 2019;288:507-11.

Journal Pre-proof

[30] Ji A, Fan YC, Ren W, Zhang S, Ai HW. A Sensitive Near-Infrared Fluorescent Sensor for Mitochondrial Hydrogen Sulfide. ACS Sens 2018;3:992-7.

[31] Xiong JC, Xia LL, Huang QL, Huang JX, Gu YQ, Wang P. Cyanine-based NIR fluorescent probe for monitoring $H_2S$ and imaging in living cells and in vivo. Talanta 2018;184:109-14.

[32] Gong SY, Zhou EB, Hong JX, Feng GQ. Nitrobenzoxadiazole ether-based near-infrared fluorescent probe with unexpected high selectivity for $H_2S$ imaging in living cells and mice. Anal Chem 2019;91:13136-42.

[33] Li QY, Wang ZC, Zhao M, Hong YP, Jin QW, Yao SY, Zheng CL, Quan YY, Ye XX, Huang ZS. A NIR fluorescent probe for the detection and visualization of hydrogen sulfide in colorectal cancer cell. Sens Actuators B 2019; doi.org/10.1016/j.snb.2019.126898.

[34] Tait SW, Green DR. Mitochondria and cell death: outer membrane permeabilization and beyond. Nat Rev Mol Cell Biol 2010;11:621-32.

[35] Smith, R.A.; Hartley, R. C.; Murphy, M. P. Mitochondria-targeted small molecule therapeutics and probes. Antioxid. redox Sign 2011;15:3021-38.

[36] Duchen MR. Mitochondria in health and disease: perspectives on a new mitochondrial biology. Mol aspects Med 2004;25:365-451.

[37] Xu W, Teoh CL, Peng JJ, Su DD, Yuan L, Chang YT. A mitochondria-targeted ratiometric fluorescent probe to monitor endogenously generated sulfur dioxide derivatives in living cells. Biomaterials 2015;56:1-9.

[38] Sun QX, Collins R, Huang S, Holmberg-Schiavone L, Anand GS, Tan CH, van-den-Berg S, Deng LW, Moore PK, Karlberg T, Sivaraman J. Structural basis for the inhibition mechanism of human cystathionine γ-lyase, an enzyme responsible for the production of $H_2S$. Biol Chem 2009;284:3076-85.

[39] Zhong KL, Deng LL, Zhao J, Yan XM, Sun T, Li JR, Tang LJ. A novel near-infrared fluorescent probe for highly selective recognition of hydrogen sulfide and imaging in living cells. RSC Adv 2018;8:23924-9.

Journal Pre-proof

[40] Li XW, Wang AN, Wang JV, Lu JZ. Efficient strategy for the synthesis and modification of 2-hydroxyethylluciferin for highly sensitive bioluminescence imaging of endogenous hydrogen sulfide in cancer cells and nude mice. Anal Chem 2019;91:15703-8.

[41] Jia Y, Xia L, Chen L, Guo XF, Wang H, Zhang HJ. A novel BODIPY-based fluorescent probe for selective detection of hydrogen sulfide in living cells and tissues. Talanta 2018;181:104-11.

[42] Fang T, Jiang XD, Sun CL, Li Q. BODIPY-based naked-eye fluorescent on-off probe with high selectivity for $H_2S$ based on thiolysis of dinitrophenyl ether. Sens. Actuators B Chem 2019;290:551-7.

[43] Liu TY, Xu ZC, Spring DR, Cui JN. A lysosome-targetable fluorescent probe for imaging hydrogen sulfide in living cells. Org Lett 2013;15:2310-3.

[44] Guria U N, Maiti K, Ali SS, Samanta SK, Mandal D, Sarkar R, Datta P, Ghoshd AK, Mahapatra AK. Reaction-based bi-signaling chemodosimeter probe for selective detection of hydrogen sulfide and cellular studies. New J Chem 2018;42:5367-75.

[45] Yuan L, Zuo QP. FRET-based mitochondria-targetable dual-excitation ratiometric fluorescent probe for monitoring hydrogen sulfide in living cells. Chem Asian J 2014;9:1544-9.

[46] Yang YT, Zhou TT, Jin M, Zhou KY, Liu DD, Li X, Huo FJ, Li W, Yin CX. Thiol−chromene “click” reaction triggered self-immolative for NIR visualization of thiol flux in physiology and pathology of living cells and mice. J Am Chem Soc 2020;142:1614-20.

[47] Li SJ, Li YF, Liu HW, Zhou DY, Jiang WL, Yang JO, Li CY. A dual-response fluorescent probe for the detection of viscosity and $H_2S$ and its application in studying their cross-talk influence in mitochondria. Anal Chem 2018;90:9418-25.

Journal Pre-proof

**Figure captions**

**Scheme 1** (a) (a) Design and (b) synthesis route of **Mito-DNP**.

**Scheme 2** Proposed detection mechanism.

**Figure 1** The UV-vis absorption and fluorescence spectra of **Mito-DNP** in the presence of $H_2S$ (10 equiv.) in PBS buffer with 50 % DMF, excited with 680 nm.

**Figure 2** (a) The UV-vis absorption and (b) fluorescence spectral changes of **Mito-DNP** (10 μM) upon addition of $H_2S$ (0-10 equiv.), excited at 680 nm.

**Figure 3** (a) Fluorescence spectral of probe **Mito-DNP** (10 μM) with various analytes (200 μM of each unless otherwise stated) in the DMF-PBS buffer (10 mM, pH 7.4, v: v = 1: 1), such as (1) none, (2) $F^-$, (3) $SCN^-$, (4) $I^-$, (5) $Br^-$, (6) $NO_3^-$, (7) $HSO_3^-$, (8) $NO_2^-$, (9) $SO_4^{2-}$, (10) $CO_3^{2-}$, (11) $ClO^-$, (12) $Cl^-$, (13) $H_2O_2$, (14), $N_3^-$, (15) $K^+$, (16) $Ba^{2+}$, (17) $Ca^{2+}$, (18)$Mg^{2+}$, (19)$Al^{3+}$, (20)$Cu^{2+}$, (21) Hcy, (22) Cys, (23) 1mM GSH, (24) 100μM $Na_2S$. (b) The changes of corresponding fluorescence intensity at 741 nm, excited at 680 nm.

**Figure 4** Intracellular localization of **Mito-DNP** in living cells. (A) HepG2 cells were incubated with 10 μM of Mito Tracker Green ($\lambda_{ex}$ = 488 nm, $\lambda_{em}$ = 490−624 nm). (B) HepG2 cells were incubated with 20 μM of $Na_2S$ and following by 10 μM of **Mito-DNP** ($\lambda_{ex}$ = 633 nm, $\lambda_{em}$ = 638−747 nm). (C)The merged images. (D) The image of bright-field. (E) The corresponding intensity profiles. (F) colocalization coefficient of MitoTracker green and **Mito-DNP**. Scale bar: 10 μm.

**Figure 5** (a) Images of exogenous $H_2S$ in living cells. (A-D) The HepG2 cells were pretreated with $Na_2S$ (0, 20, 50, 100 μM), following by **Mito-DNP** (10 μM). (E) The corresponding fluorescence intensity. (b) Images of endogenous $H_2S$ in live cells. (A-D) The cells were respectively pretreated with none, PAG (200 μM), Cys (100 μM), Cys (100 μM) and PAG (200 μM), then incubated with **Mito-DNP** (10 μM). (E) The corresponding fluorescence intensity. (λex = 633 nm, λem = 638−747 nm), Scale bar: 10 μm.

**Figure 6** Images of $H_2S$ in BALB/c Nude Mice. (A) The mice incubated with **Mito-DNP** (0.2mM, 100μL) for 30min, (B) The mice preincubated with **Mito-DNP**

(0.2mM, 100μL) for 30min after injection of Cys (2mM,100μL) for 30min, (C) The mice preincubated with **Mito-DNP** (0.2mM, 100μL) for 30 min after injection of PAG (2mM, 200μL) and Cys (2mM,100μL) for 30 min, (D) The image of the mice incubated with **Mito-DNP** (0.2mM, 100μL) for 30min after injection of $Na_2S$ (2 mM, 100μL). excited at 680 nm.

**Scheme 1**

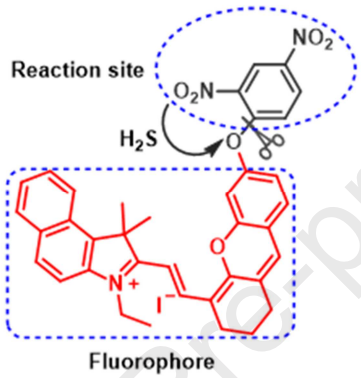


(a)

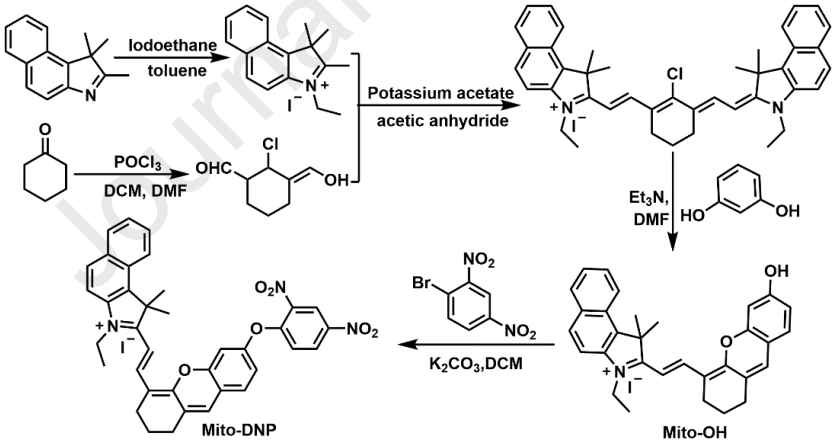


(b)

**Scheme 2**

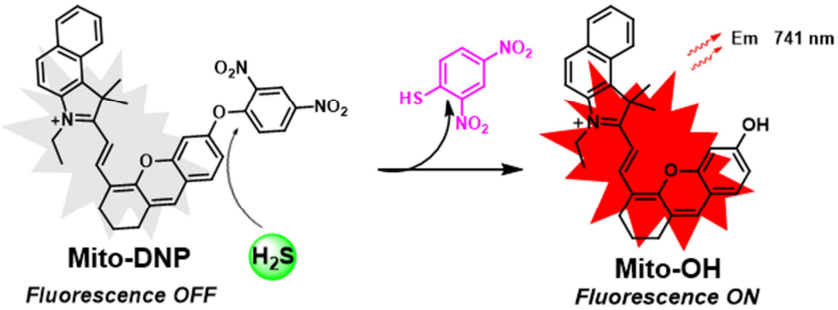

**Figure 1**

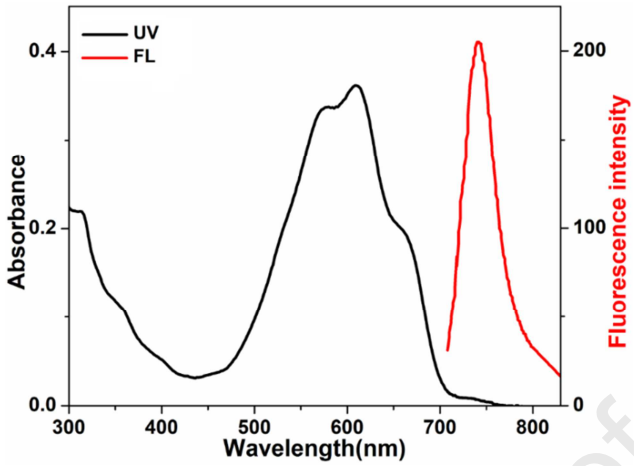


**Figure 2**

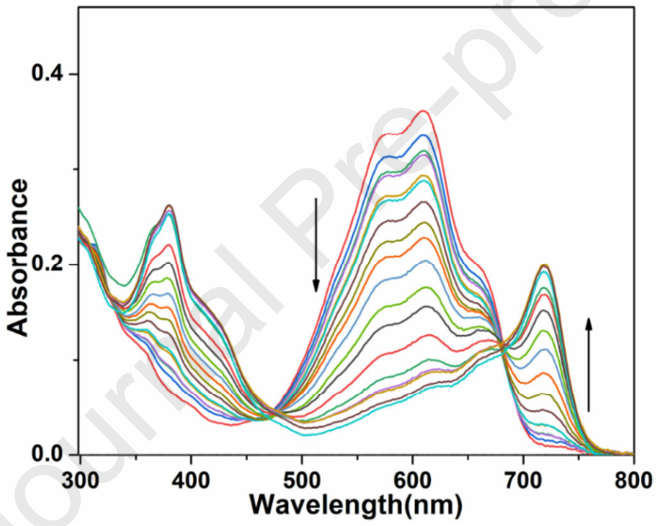


(a)

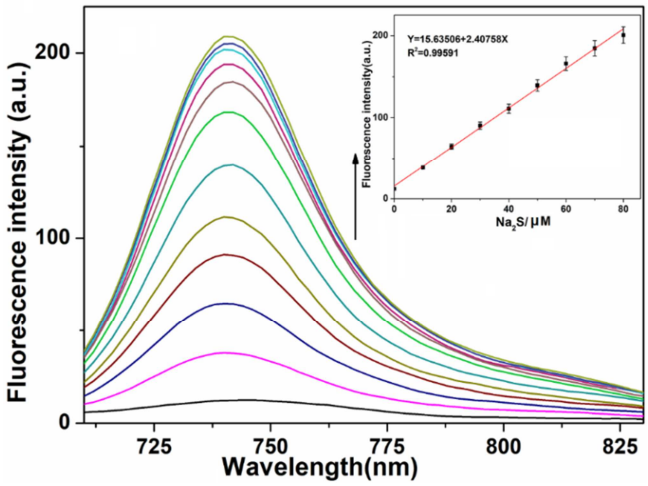


(b)

Journal Pre-proof

**Figure 3**

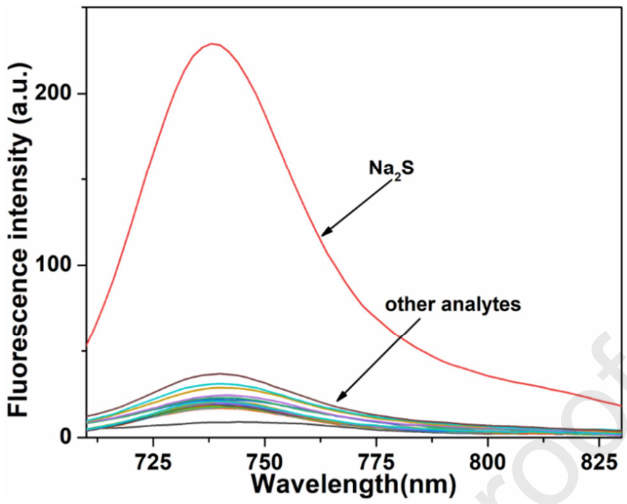


(a)

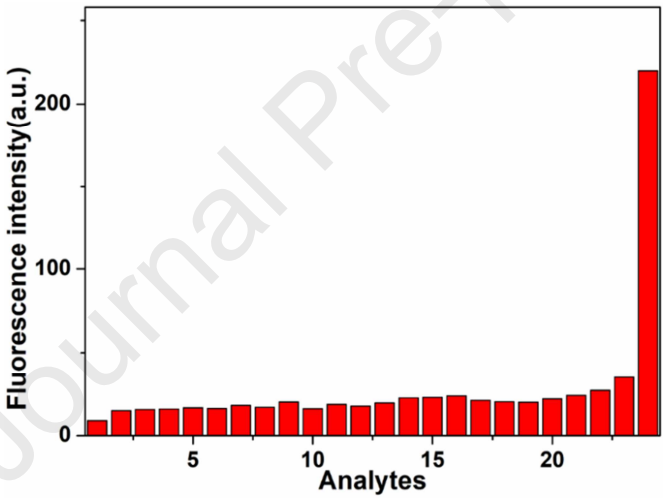


(b)

**Figure 4**

Journal Pre-proof

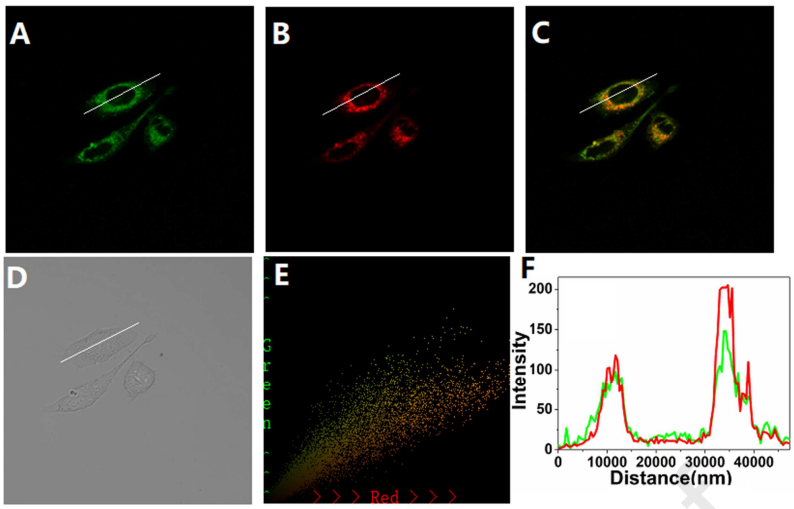


**Figure 5**

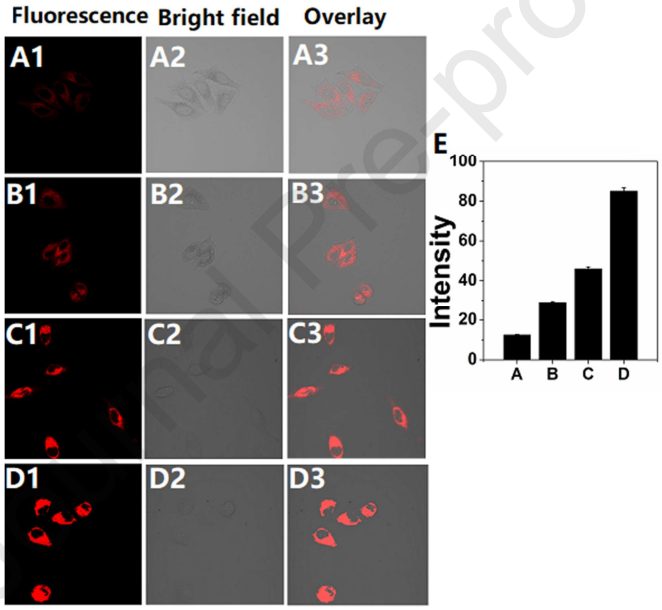


(a)

Journal Pre-proof

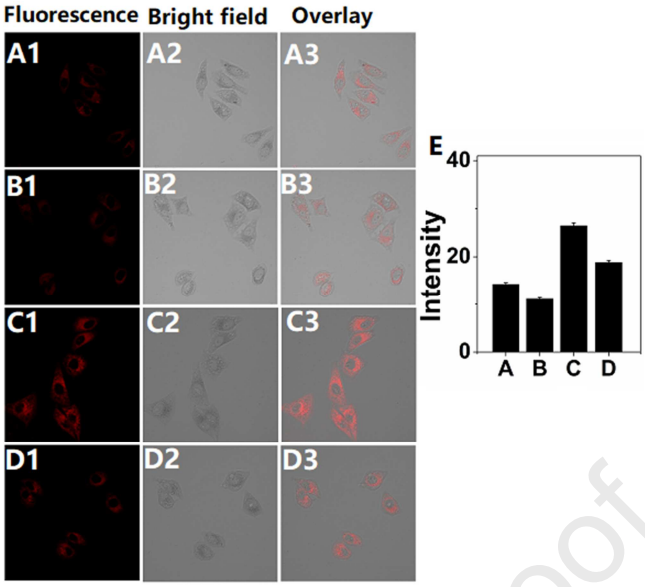


(b)

**Figure 6**

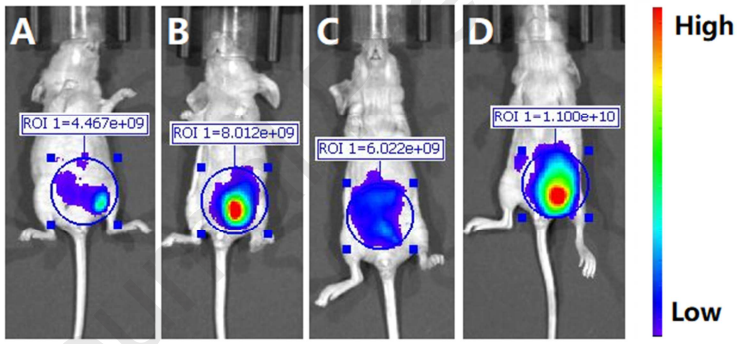


Journal Pre-proof

Journal Pre-proof

# Highlights

1. A multifunctional and high efficient hydrogen sulfide NIR fluorescent probe was developed.
2. Strong electrophilic group was selected to promote the nucleophilic substitution reaction
3. The probe demonstrated excellent performance in the detection hydrogen sulfide in *vivo*.

Journal Pre-proof

Journal Pre-proof

# Supporting Information

**Figure captions**

Figure S1: Reaction time profile of the probe **Mito-DNP** and towards $Na_2S$.

Figure S2: Choice of pH range for the measurements.

Figure S3: Competing experiments.

Figure S4: HRMS spectra.

Figure S5: MTT assay.

Figure S6: NMR spectra.

Table S1 Comparison of fluorescent probes for $H_2S$.

Journal Pre-proof

**Figure S1:** Reaction time profile of the probe **Mito-DNP** and towards $Na_2S$.

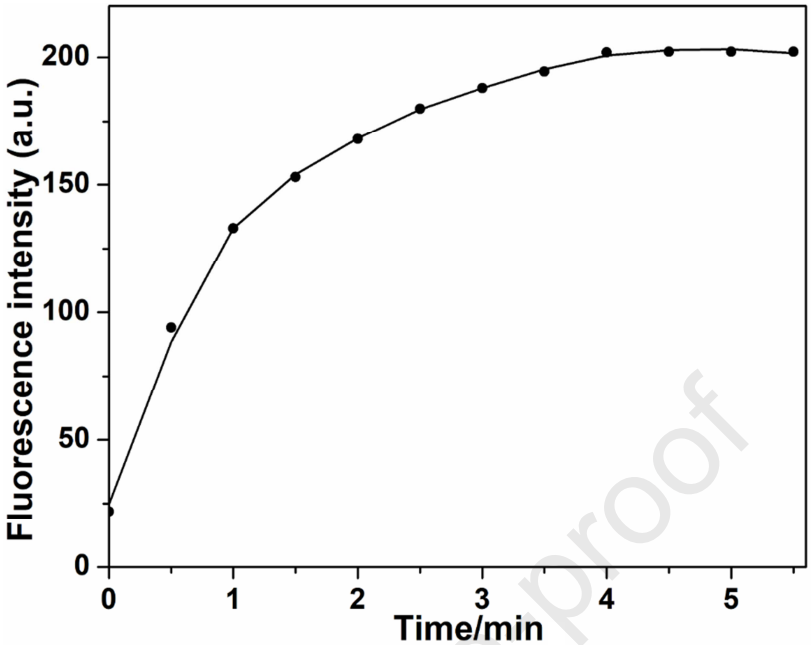


**Figure S1**: Reaction time profile of the probe **Mito-DNP** (10 μM) and towards $Na_2S$ (100 μM) at 741 nm ( $\lambda_{Ex}$ = 680 nm, $\lambda_{Em}$ = 741 nm, slit: 5 nm/5 nm).

**Figure S2: Choice of pH range for the measurements.**

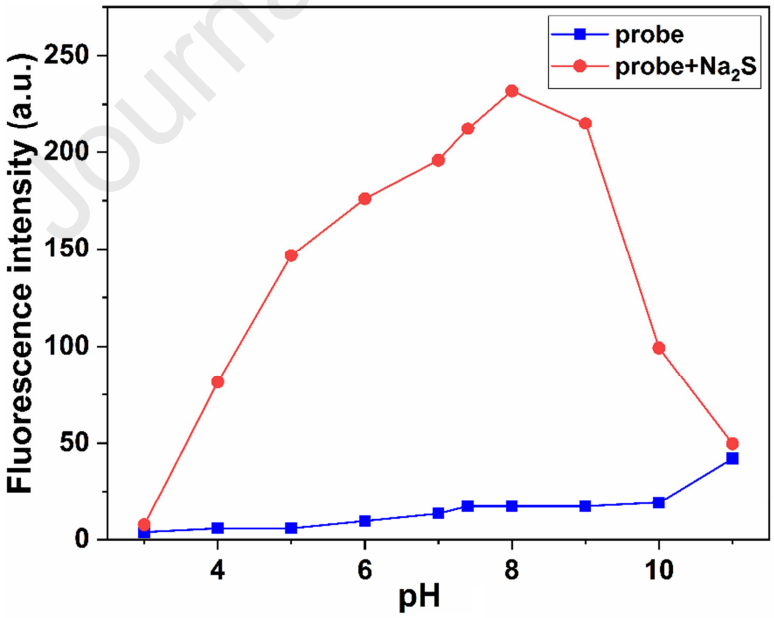


**Figure S2**: Effect of pH on the fluorescence intensity of **Mito-DNP** (10 μM) in DMF-PBS buffer (10mM, pH7.4, v:v=1:1). Concentration of sodium sulfide: (a) 0 μM, (b) 100 μM.

Figure S3 Competing experiments.

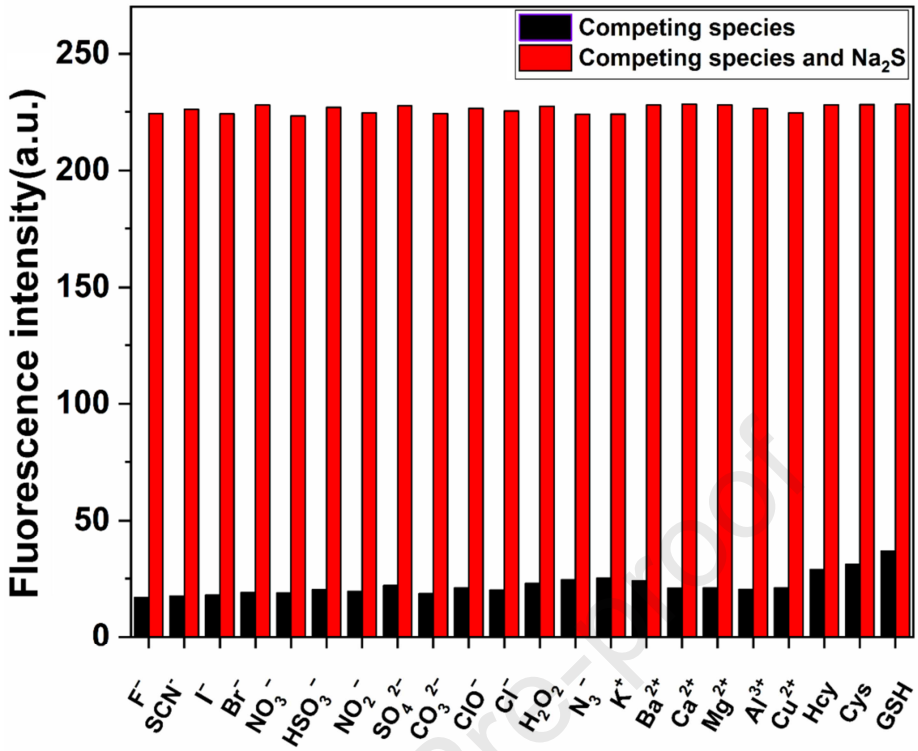


Figure S3 Fluorescence intensity ($\lambda_{em}$= 680 nm) changes of the probe **Mito-DNP** (10 μM) in DMF- PBS buffer (10mM, pH7.4, v:v=1:1) solution upon addition of various species.

**Figure S4: MTT assay**

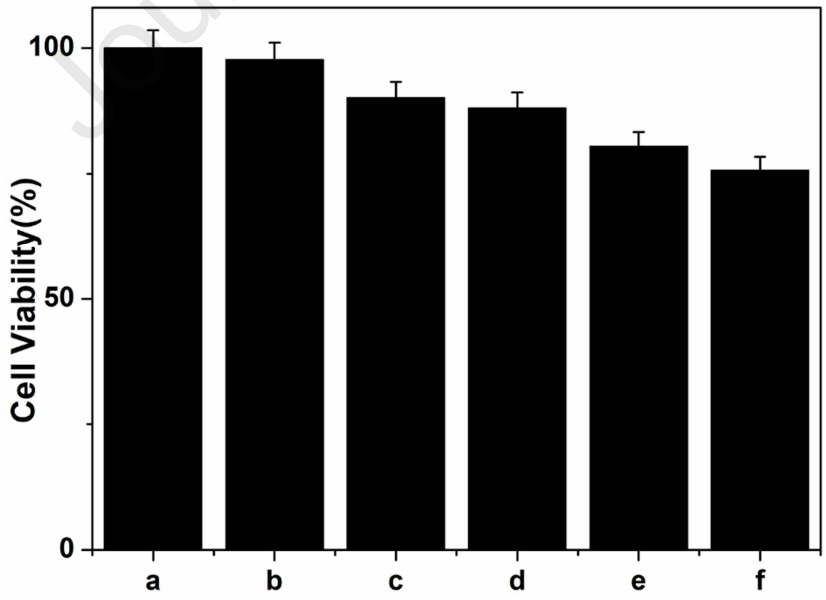

**Figure S4:** MTT assay to determine the survival rate of different concentrations of **Mito-DNP** (a-f：0μM、2μM、5μM、10 μM、15μM、20μM) on HepG2 cells for 12 h.

**Figure S5: HRMS spectra**

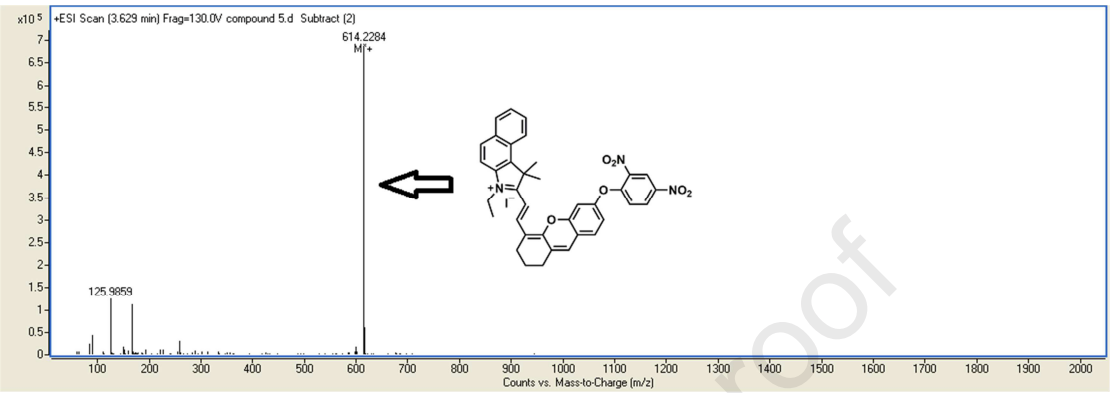


HRMS of **Mito-DNP.**

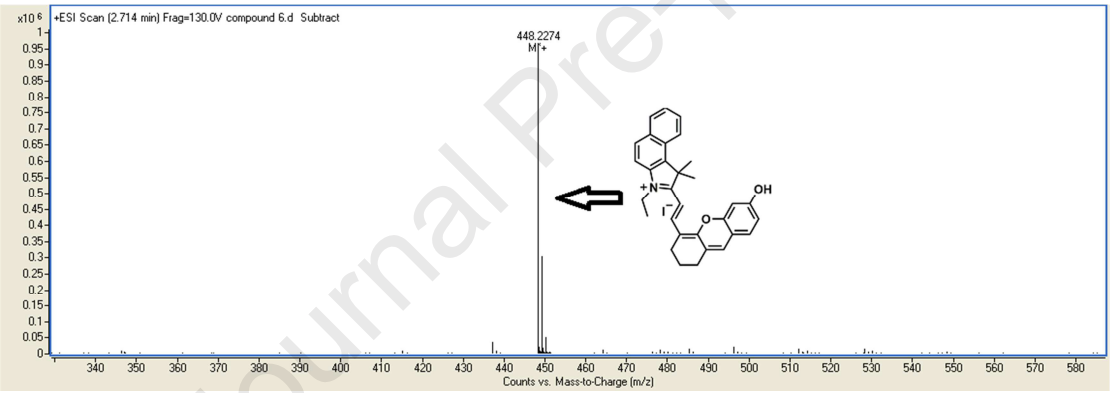


HRMS of **Mito-OH.**

**Figure S6: NMR spectra**

Journal Pre-proof

Journal Pre-proof

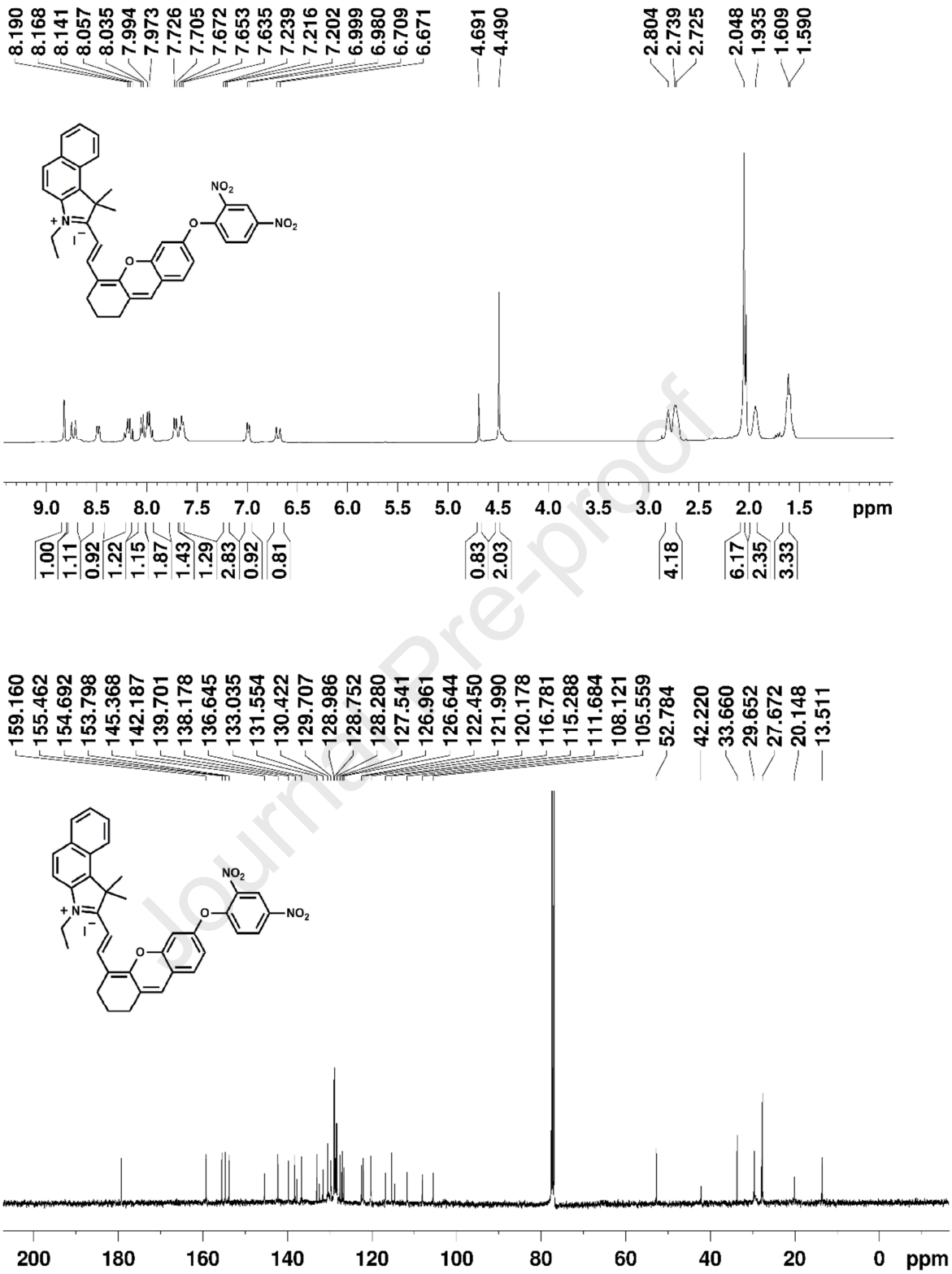


$^{1}$H NMR and $^{13}$C NMR of probe **Mito-DNP** in $CDCl_3$.

Table S1 Comparison of fluorescent probes for $H_2S$.

| probe | λex/λem | Detection | Detection | Response | Ref |
|---|---|---|---|---|---|

| | (nm) | medium | limit | time | |
|---|---|---|---|---|---|
| 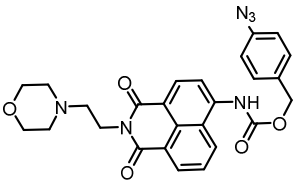 | 410/541 | PBS/$CH_3CN$ =4:1 (v/v) solution | 0.70 μM | 2 h | 1 |
| 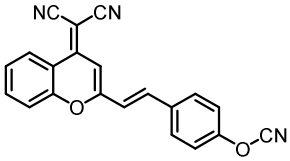 | 550/690 | PBS buffer solution (10mM PBS, CTAB 4 mM, pH 7.4). | 0.28 μM | 3 min | 2 |
| 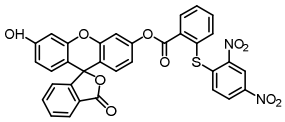 | 512/538 | DMSO: PBS (v/v, 7 : 3, pH=7.4) solution | 64 nM | 600 s | 3 |
| 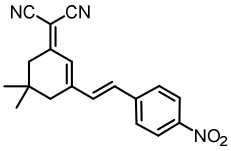 | 510/650 | PBS buffer solution (pH 7.4) | 1.08 nM | 60 s | 4 |
| 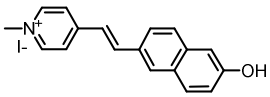 | 410/575 | BR buffer solution ($H_2O$; pH=7.42, 40 mM) | 11.2 nM | 15 min | 5 |
| 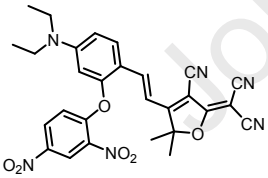 | 543/660 | DMF/$H_2O$ (3:7, v/v, PBS 10 mM, pH = 7.4) | 3.09 μM | 170 min | 6 |
| 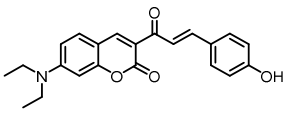 | 470/556 | EtOH/$H_2O$ medium (2 mL, pH ~ 7, 1:1, v/v) | 50 nM | 60 s | 7 |
| 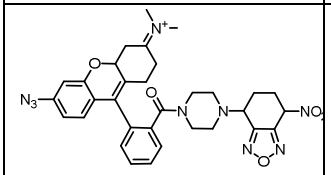 | 488/565 | PBS buffer (20 mM, pH 7.4) | 120 nM | 20 min | 8 |
| 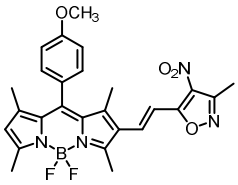 | 448/522 | buffer PBS-DMSO (9:1 v/v, pH 7.4) | 2.55 μM | 55 s | 9 |

Journal Pre-proof

| | | | | | |
|---|---|---|---|---|---|
| 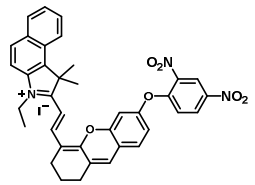 | 680/741 | DMF-PBS (10 mM, pH 7.4, v:v =1:1) buffer solution | 96 nM | 4 min | This work |

**References**


[1] Feng WQ, Mao ZQ, Liu LZ, Liu, ZH. A ratiometric two-photon fluorescent probe for imaging hydrogen sulfide in lysosomes. Talanta 2017;167:134-42.

[2] Jin YL, Liu R, Zhan ZX, Lv Y. Fast response near-infrared fluorescent probe for hydrogen sulfide in natural waters. Talanta 2019;202:159-64.

[3] Kang J, Huo FJ, Yao YS, Yin CX. A high signal-to-background ratio $H_2S$-specific fluorescent probe base on nucleophilic substitution and its bioimaging for generation $H_2S$ induced by $Ca^{2+}$ in vivo. Dyes Pigments 2019; doi.org/10.1016/j.dyepig.2019.107755.

[4] Wu Q, Yin CX, Wen Y, Zhang YB, Huo FJ. An ICT lighten ratiometric and NIR fluorogenic probe to visualize endogenous/exogenous hydrogen sulphide and imaging in mice. Sens Actuators B 2019;288:507-11.

[5] Chen G, Xu J, Zhan ZH, Gao XY, Jiao MQ, Ren MZ, Lv LH, Chen T, Li YL, Liu YX. A bright two-photon fluorescence probe with large stokes shift for deep tissue imaging of $H_2S$ during metabolism. Dyes Pigments 2020; doi.org/10.1016/j.dyepig.2019.107850.

[6] Zhong KL, Chen L, Pan YX, Yan XM, Hou SH, Tang YW, Gao X, Li JR, Tang LJ. A colorimetric and near-infrared fluorescent probe for detection of hydrogen sulfide and its real multiple applications. Spectrochim Acta A 2019; doi.org/10.1016/j.saa.2019.117135.

[7] Yang Y, Feng Y, Jiang Y, Qiu FZ, Wang YZ, Song XR, Tang XL, Zhang GL, Liu WS. A coumarin-based colorimetric fluorescent probe for rapid response and highly sensitive detection of hydrogen sulfide in living cells. Talanta 2019;197:122-9.


Journal Pre-proof

[8] Ma C, Wei C, Li XY, Zheng XY, Chen B, Wang M, Zhang PZ, Li XL. A mitochondria-targeted dual-reactable fluorescent probe for fast detection of $H_2S$ in living cells. Dyes Pigments 2019;162:624-31.

[9] Zhou N, Yin CX, Chao JB, Zhang YB, Huo FJ. An isoxazole-accelerated nitro oxidation type fluorescent detection and imaging for hydrogen sulfide in cells. Sens Actuators B 2019;287:131-7.

Journal Pre-proof

Journal Pre-proof

# Declaration of interest statement

We have no any interest conflict.

Journal Pre-proof